How Can Knowledge of a Task's Modular Structure Improve Generalization and Training Efficiency?

Shreyas Malakarjun Patil *sm_patil@gatech.edu*
School of Computer Science, Georgia Institute of Technology

Cameron Taylor *cameron.taylor@gatech.edu*
School of Computer Science, Georgia Institute of Technology

Constantine Dovrolis *constantine@gatech.edu, c.dovrolis@cyi.ac.cy*
School of Computer Science, Georgia Institute of Technology
Computational Science and Technology Research Center (CaSToRC), The Cyprus Institute

Reviewed on OpenReview: *https://openreview.net/forum?id=46hFTOUox7*

Abstract

Many real-world learning tasks have an underlying hierarchical and modular structure, composed of smaller sub-functions. Traditional neural networks (NNs) often disregard this structure, leading to inefficiencies in learning and generalization. Prior work has demonstrated that leveraging known structural information can enhance performance by aligning NN architectures with the task's inherent modularity. However, the extent of prior structural knowledge required to achieve these performance improvements remains unclear. In this work, we investigate how modular NNs can outperform traditional dense NNs on tasks with simple yet known modular structure by systematically varying the degree of structural knowledge incorporated. We compare architectures ranging from monolithic dense NNs, which assume no prior knowledge, to hierarchically modular NNs with shared modules that leverage sparsity, modularity, and module reusability. Our experiments demonstrate that module reuse in modular NNs significantly improves learning efficiency and generalization. Furthermore, we find that module reuse enables modular NNs to excel in data-scarce scenarios by promoting functional specialization within modules and reducing redundancy.

1 Introduction

Real-world learning tasks often exhibit an inherent hierarchical and modular structure, where a complex target function can be decomposed into smaller, hierarchically organized sub-functions (Simon, 1991). Traditional neural networks (NNs), such as multilayered perceptrons (MLPs), however, treat target functions as undifferentiated input-output mappings, disregarding any underlying modular structure. This leads to higher training costs and increased data requirements. By exploiting the task structure in NN architecture design, efficiency and generalization can be significantly improved. For instance, in domains like vision and language, prior structural knowledge such as spatial locality and temporal coherence are well understood. These priors, when encoded using convolutional or recurrent architectures, are known to significantly improve generalization performance and training efficiency.

On the other hand, the precise hierarchical and modular structure underlying a given task is often unknown. To address this, previous work has explored explicit hierarchical and modular architectures that incorporate partial knowledge of the task structure (Fernando et al., 2017; Rosenbaum et al., 2017; Shazeer et al., 2017; Kirsch et al., 2018; Goyal et al., 2019; 2021; Ponti et al., 2022). These architectures break the NN into sparsely connected sub-networks or modules, each learning a distinct sub-function, and organize them hierarchically, where the organization itself is learned.

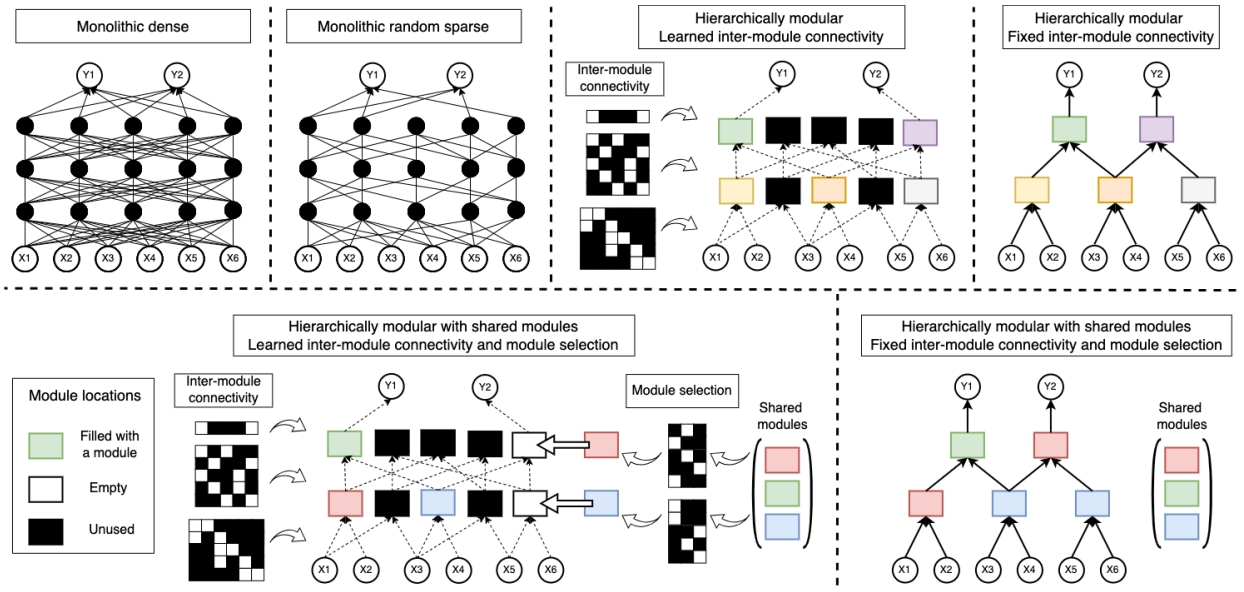

Figure 1: Overview of the models, highlighting varying levels of structural knowledge assumed at initialization. The associated task for these architectures is depicted in Figure 2 (depth 2). From top left to bottom right: Monolithic dense NN: Unknown task structure. Monolithic random sparse NN: Sparsity in task structure. Hierarchically modular NN: Modular sparsity pattern. Hierarchically modular NN (fixed inter-module connectivity): Modular sparsity with known sub-function connectivity. Hierarchically modular NN with shared modules: Modular sparsity and module reusability. Hierarchically modular NN with shared modules (fixed inter-module connectivity and module selection): Modular sparsity, module reusability, known sub-function connectivity and reuse.

The variety of specific architectural choices tailored to different tasks raise questions about the extent of prior knowledge required for performance improvements. For instance, architectures designed for tasks like visual question answering (VQA) often depend on a high degree of prior knowledge about the task's modularity (Andreas et al., 2016; Hu et al., 2017). Conversely, generic configurations like mixture-of-experts (MoE) or routing networks excel in domains such as multi-task learning (Rosenbaum et al., 2017; Purushwalkam et al., 2019; Hazimeh et al., 2021; Ponti et al., 2022; Chen et al., 2023), transfer / continual learning (Terekhov et al., 2015; Wang et al., 2020; Veniat et al., 2020; Mendez & Eaton, 2020; Ostapenko et al., 2021), and compositional generalization (Bahdanau et al., 2018; Lake & Baroni, 2018; Chang et al., 2018; Hupkes et al., 2020; Rahaman et al., 2021). In these domains, where sub-functions are dynamically organized or selected based on input-dependent cues, modular designs enable flexible function representation by adapting the organization or selection of modules for different inputs. Even in these settings, previous analysis suggests that knowing specific input components influencing module organization (Mittal et al., 2022), as well as understanding module architecture (such as input dimensions) or identifying input bottlenecks, improves generalization (Bahdanau et al., 2019; Goyal et al., 2021; Ostapenko et al., 2022).

Our work contributes to this line of inquiry (Pathak et al., 2019; D'Amario et al., 2021; Mittal et al., 2022; Ostapenko et al., 2022; Schug et al., 2023; Jarvis et al., 2024; Lippl & Stachenfeld, 2024) by systematically studying how different degrees of structural knowledge impact NN generalization and training efficiency. We consider tasks with fixed and known hierarchically modular structure, particularly those derived from Boolean functions. Unlike prior works that focus on input-dependent modular structure, a static modular structure provides a controlled environment for evaluating key architectural principles such as sparsity, modularity, and module reusability, while isolating those factors from principles used to learn input-dependent hierarchical organization. Additionally, the synthetic Boolean tasks with completely known structure allows for systematically varying the degree of prior knowledge encoded in the architecture, from assuming no prior knowledge to complete structural knowledge.

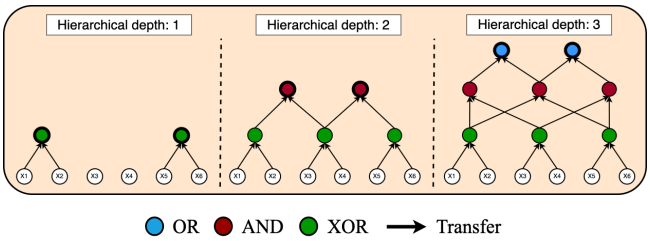

Figure 2: Function graphs with varying complexity used to generate the truth tables.

We start with dense NNs that make no structural assumptions, followed by random sparse NNs that assume sparsity without a specific pattern, classifying them as monolithic NNs. We then examine hierarchically modular NNs, where modules are explicitly defined and organized hierarchically (Fernando et al., 2017; Ostapenko et al., 2021). In these networks, both module weights and inter-module connections are learned without assuming prior knowledge of specific connectivity. We extend this exploration to modular NNs with fixed inter-module connectivity, where the exact sub-function connectivity is known. Finally, we introduce module reusability, where the same module can be used in multiple locations within the hierarchy, reflecting the idea that sub-functions may recur throughout the task (Goyal et al., 2021; Ostapenko et al., 2022). In this setup, the NN must dynamically learn both connectivity and module selection from a shared pool of modules. We also explore a variant with fixed connectivity and module selection, representing complete structural knowledge.

All architectures studied are implemented using multi-layer perceptrons (MLPs) and involve learning functional components, regardless of the degree of structural knowledge incorporated. We systematically analyze the effects of sparsity, modularity, and module reusability on generalization and training efficiency. Our findings demonstrate that hierarchically modular NNs with shared modules consistently outperform dense NNs, especially in data-scarce scenarios. Furthermore, module reuse through sharing facilitates the accurate learning of inter-module connectivity while promoting functional specialization within modules, ultimately leading to improved generalization. These results are demonstrated on simple, hierarchically modular tasks with fully known structure, primarily Boolean functions and are further validated on a visual recognition task using the MNIST dataset.

2 Preliminaries

2.1 Hierarchically Modular Boolean Functions

In this work, we construct hierarchical and modular tasks using Boolean functions (Malakarjun Patil et al., 2024). A Boolean function $f : \{0,1\}^n \rightarrow \{0,1\}^m$ maps n input bits to m output bits. The set of gates G includes $\{\wedge, \vee, \oplus\}$ (AND, OR, XOR), with edges representing direct connections.

A *function graph* for a Boolean function is represented as a directed acyclic graph (DAG) consisting of n input nodes with zero in-degree, k gate nodes with non-zero in-degree (associated with gates from G), and m output nodes with zero out-degree. A *truth table* is a tabular representation of a Boolean function that enumerates all possible input combinations and their corresponding outputs.

A *sub-function* or sub-task corresponds to a gate node within the function graph that applies an operation on its specific inputs. Sub-functions are organized hierarchically, with outputs from certain sub-functions serving as inputs for others. These sub-functions have three fundamental properties:

1. *Input Connectivity and Separability:* Sub-functions operate on outputs from previous sub-functions or input nodes. This connectivity is sparse—each sub-function relies on a subset of preceding outputs. In our experiments, each sub-function takes exactly two inputs to maintain uniformity across graphs.

2. *Output Connectivity and Reusability:* Outputs produced by a sub-function can be reused by multiple sub-functions at higher hierarchical levels, similar to feature reuse in NNs.

3. *Sub-Function Reusability:* The functional operation of a sub-function can be reused at multiple locations in the function graph. For instance, an XOR gate might be reused in various parts of the graph.

A task's hierarchical structure or *sub-function organization* is defined by the relationships among these underlying sub-functions.

2.2 Neural Network Architectures

In this section we describe various NN architectures used in our experiments.

Monolithic NNs: We consider dense multi-layer perceptrons (MLPs) and sparse MLPs. Sparse MLPs are created by random pruning to introduce sparsity, leveraging a notion of sparsity in the function graph but without its specific pattern.

Hierarchically Modular NNs (*modular*): The *modular* architecture is arranged in L hierarchical layers, each containing M_l modules, denoted as m_l^i, where i represents the module's position within layer l. Each module includes a small MLP and an input selection vector $\boldsymbol{s}_l^i \in \mathbb{R}^{M_{l-1}}$. The MLP learns the functional component, while the input selection vector governs inter-module connectivity by selecting module inputs from the outputs of modules in the previous layer. The final outputs of the NN are selected from the set of all modules in the last layer using an output selection vector.

We explore two scenarios: 1. *Modular:* Both inter-module connectivity and module MLP weights are learned. 2. *Modular-FC:* Inter-module connectivity is fixed, inferred from the function graph, while module MLP weights are learned.

Learning Inter-Module Connectivity: Given outputs from layer $l-1$, $\boldsymbol{x}_{l-1} \in \mathbb{R}^{M_{l-1}}$, the Sigmoid function is applied to $\boldsymbol{s}_l^i$ to produce a score for each potential input, selecting the top-k inputs. We use the straight-through estimator (Bengio et al., 2013) to propagate gradients through non-differentiable selections, facilitating effective learning of inter-module connectivity. See Appendix A for additional implementation details and Appendix F.1 for experiments related to learning inter-module connectivity.

Hierarchically Modular NNs with Shared Modules (*modular-shared*): The *modular-shared* architecture extends the *modular* architecture, treating module positions as slots filled by modules from a shared pool of M modules. Each slot has an input selection vector $\boldsymbol{s}_l^i \in \mathbb{R}^{M_{l-1}}$ and a module selection vector $\boldsymbol{v}_l^i \in \mathbb{R}^M$, which determines the module used in that slot. The final outputs are selected from the set of slots in the last layer using an output selection vector.

We explore two scenarios: 1. *Modular-shared:* The network learns both inter-module connectivity and module selection dynamically, alongside module weights. 2. *Modular-shared-FCMS:* Connectivity and module selection are fixed, with only the module weights being learned.

Learning Inter-Module Connectivity and Module Selection: Outputs from slots at layer $l-1$, $\boldsymbol{x}_{l-1} \in \mathbb{R}^{M_{l-1}}$, are selected as inputs similar to the previous architecture. The chosen inputs are passed to a module determined by the selection vector $\boldsymbol{v}_l^i \in \mathbb{R}^M$, which is first transformed via a Softmax function to assign probabilities to each module in the shared pool. The module with the highest probability is selected (top-1). The straight-through estimator is used to compute gradients for both $\boldsymbol{s}_l^i$ and $\boldsymbol{v}_l^i$ (see Appendix A).

Hereafter, "hierarchically modular NNs" refers to both *modular* and *modular-shared* unless otherwise specified.

3 Learning Modular Boolean Tasks

We evaluate the performance of different NN architectures by learning Boolean functions represented as function graphs. The truth table derived from these graphs serves as the dataset. Our evaluation focuses on the models' generalization and learning efficiency when only a fraction of the truth table is available for training.

Experiment Details: We use three function graphs, each with 6 input nodes and 2 output nodes, as depicted in Figure 2. The complexity is controlled by the number of hierarchical levels—greater depth implies increased dependence on intermediate sub-functions, making the task more intricate.

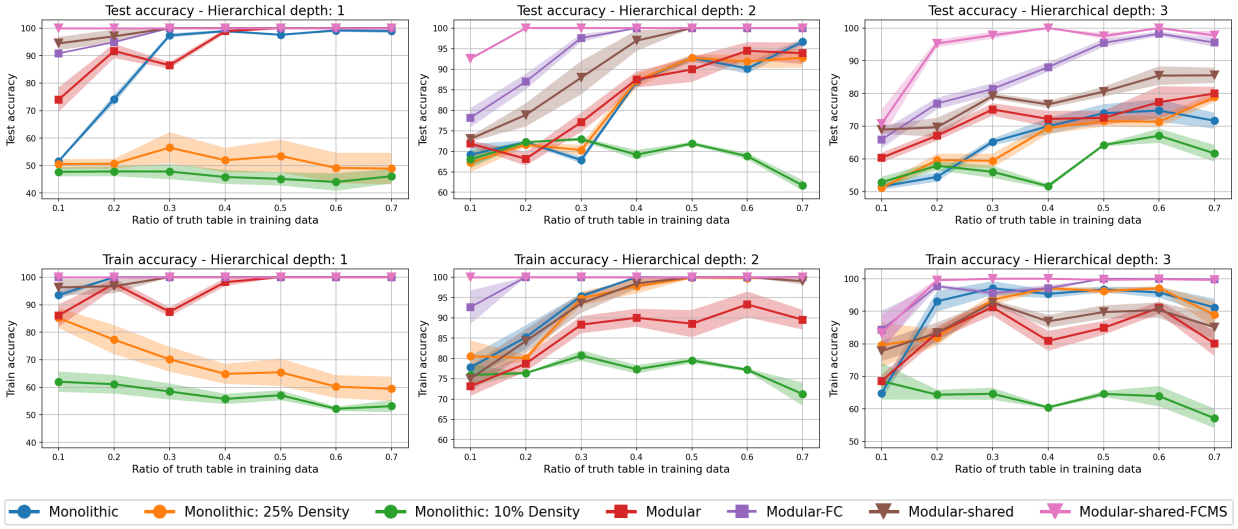

Figure 3: Test and train accuracy of different NNs relative to training size. For each datapoint, we report the mean and combined standard error (shaded region).

The NN architectures are trained on different portions of the truth table, with training sizes ranging from 0.1 to 0.7 of the total rows. The remaining rows are split evenly between validation and test sets. For each training size, we create three random partitions of the truth table, and each partition is trained with three additional random seeds, resulting in a total of nine training runs per architecture per training size. We report the mean and combined standard error, calculated from the three separate means corresponding to the three dataset partitions. To enhance robustness, random noise from $\mathcal{N}(0, 0.1)$ is added to the inputs during training for data augmentation. All models are trained using the Adam optimizer for 1000 epochs.

To ensure consistency, *modular* and *modular-FC* architectures use the same number of modules as there are gate nodes at each level of the function graph (Mittal et al., 2022). Similarly, *modular-shared* and *modular-shared-FCMS* architectures align the number of slots with the number of gate nodes, and the count of shared modules matches the number of distinct gates in the graphs. Appendix C demonstrates that varying the number of modules or slots has minimal impact on performance. All module MLPs have a uniform structure, with 2 input units, a hidden layer with 12 units, and 1 output unit. We fix the number of inputs to modules in hierarchically modular NNs to 2, ensuring structural consistency while preventing module collapse and optimizing module utilization (Goyal et al., 2021; Ostapenko et al., 2022). Additional experiments, presented in Appendix D, explore varying module input dimensions. These results demonstrate that precise knowledge of the module input size has minimal impact on generalization performance.

Monolithic NNs are configured with 1, 3, or 5 hidden layers to match the depth of the hierarchically modular NNs, with each hidden layer containing 36 units. Further architectural and training details can be found in Appendix A.

3.1 Generalization Performance

Comparing Architectures: Figure 3 shows the generalization performance of different NN architectures relative to the training size.

1. *Monolithic Dense vs. Monolithic Sparse:* The performance of monolithic NNs is heavily influenced by parameter count. As sparsity increases, test accuracy declines significantly.

2. *Modular vs. Monolithic: Modular* NNs possess only 30%, 7.1%, and 5.9% of the weights compared to monolithic dense NNs for functions with depth 1, 2, and 3, respectively. They outperform monolithic sparse NNs with similar parameter counts (see Appendix Table 1 for details). As the parameter count of monolithic

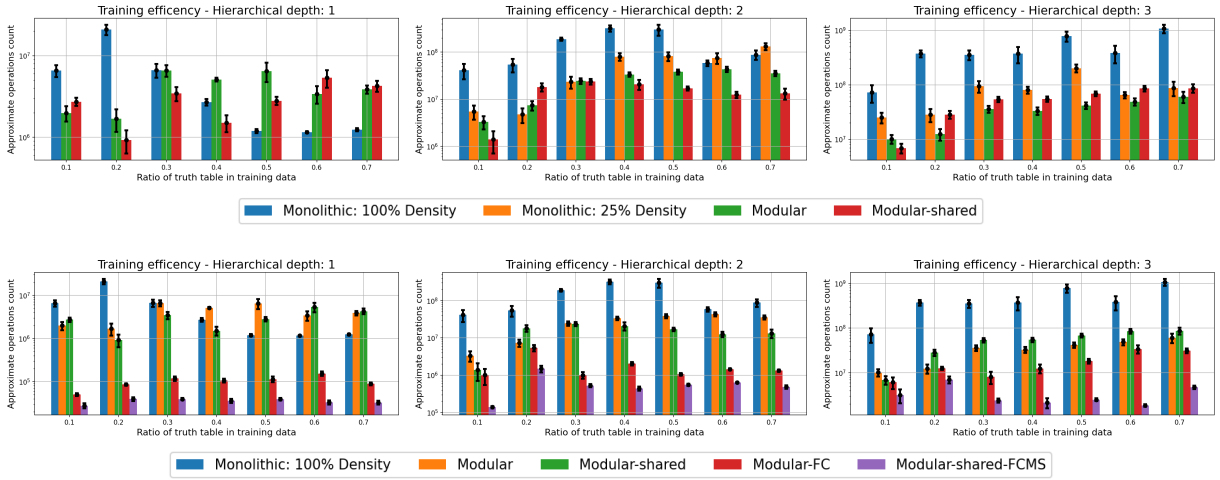

Figure 4: FLOPs required to train various NNs as compared to the ratio of truth table available.

NNs increases, their test accuracy converges with that of *modular* NNs, indicating that prior knowledge of modular sparsity is most beneficial when parameter counts are similar.

3. *Modular-Shared vs. Monolithic and Modular: Modular-shared* NNs consistently outperform both monolithic and *modular* NNs, benefiting from module reuse that artificially increases the number of samples per module and leads to efficient learning of sub-functions. For depth-1 and depth-2 functions, *modular-shared* NNs significantly outperform the others. However, for depth-3 functions, the performance gap narrows, suggesting that for highly complex tasks, the benefits of modularity and reuse diminish, especially with limited training data.

4. *Fixed Connectivity and Module Selection: Modular-FC* and *modular-shared-FCMS* NNs demonstrate superior performance compared to all other NNs. *Modular-shared-FCMS* NNs are particularly effective with minimal training data, highlighting the value of reusability and fixed structure, which reduces the complexity associated with concurrently learning both the sub-functions and their organization.

Train Accuracy vs. Test Accuracy: *Modular* and *modular-shared* NNs tend to have closely aligned train and test accuracy, while monolithic NNs often exhibit overfitting, particularly with limited training data. This suggests that the inherent inductive bias of hierarchically modular NNs effectively prevents overfitting by aligning the learned representations with the true task structure.

Generalization Relative to Function Complexity: As function complexity increases, all NNs require larger training sizes for effective generalization. A minimum threshold of training data exists for each architecture, determined by its level of prior knowledge, to generalize to unseen samples. This threshold increases with complexity, but decreases with greater structural knowledge, such as module reuse and fixed connectivity.

3.2 Training Efficiency

We next evaluate training efficiency based on the number of floating-point operations (FLOPs) required for training. FLOPs are calculated considering the number of training iterations to reach peak validation accuracy, training size, and the number of weights used in forward and backward passes, as well as in optimization updates. We compare architectures in two groups, including only those that generalize effectively (see Appendix B for further details).

Comparing Architectures: Figure 4 presents the FLOPs required for training different NNs.

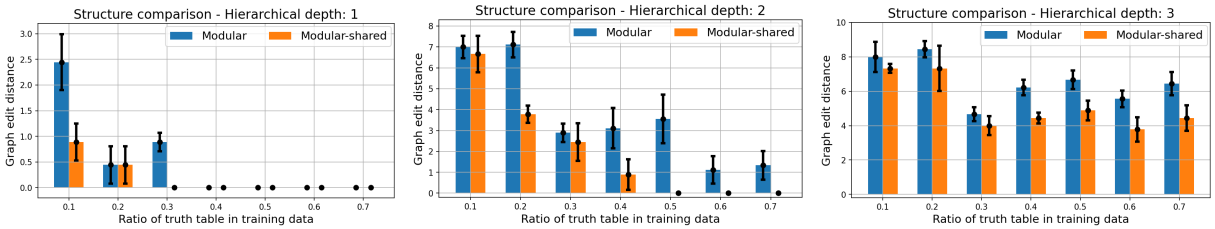

Figure 5: Minimum graph edit distance between the learned connectivity in *modular* and *modular-shared* NNs and the ground truth function graphs.

1. *Monolithic Dense vs. Monolithic Sparse:* Monolithic sparse NNs achieve better training efficiency due to reduced parameter counts. There exists a range of densities for which sparse NNs match the generalization of dense NNs while reducing training costs.

2. *Modular vs. Monolithic: Modular* NNs use only 30%, 7.1%, and 5.9% of the weights of monolithic dense NNs for depths 1, 2, and 3, respectively, leading to improved training efficiency. However, with sufficient training data, monolithic dense NNs can converge more quickly for simpler tasks, ultimately showing better efficiency, as seen for the depth-1 and depth-2 functions at high training sizes. Monolithic sparse NNs (25% density) can also match the generalization performance of *modular* NNs with similar training efficiency but lack the convergence speed-up seen in dense NNs, likely due to reduced parameterization. See Appendix B for NN convergence performance.

3. *Modular-Shared vs. Monolithic and Modular: Modular-shared* NNs consistently demonstrate superior training efficiency compared to monolithic dense NNs, although dense NNs eventually catch up with increasing training size for simpler tasks. *Modular-shared* NNs require similar FLOPs to monolithic sparse and *modular* NNs but outperform them in generalization.

Also, hierarchically modular NNs do not achieve faster convergence with larger training size – possibly because they need to explore and determine the inter-module connectivity.

4. *Fixed Connectivity and Module Selection: Modular-FC* and *modular-shared-FCMS* NNs achieve the highest training efficiency. *Modular-shared-FCMS* NNs perform particularly well, underscoring the computational advantage of focusing on learning only the sub-functions as compared to learning the sub-functions along with exploring and determining their organization. Further analysis in Appendix F.2 shows that structural parameters require higher learning rates than module MLPs.

Efficiency Relative to Function Complexity: As function complexity increases, training all architectures requires more operations. For low-complexity functions, monolithic dense NNs are more efficient compared to others. However, as complexity grows, NNs with prior structural knowledge (e.g., sparsity, modularity, and reuse) achieve better efficiency. This improvement is directly tied to their ability to generalize effectively as compared to dense NNs with increasing task complexity. *Modular-FC* and *modular-shared-FCMS* NNs particularly benefit from prior knowledge of connectivity and module selection, significantly enhancing training efficiency.

3.3 Factors Influencing Generalization in Modular NNs

In this section, we analyze two key factors influencing the generalization of *modular* and *modular-shared* NNs: learning the sub-function organization through inter-module connectivity and achieving functional specialization within modules, particularly under limited data conditions.

Learning the Sub-Function Organization: Unlike monolithic dense NNs, which directly learn input-output mappings, *modular* and *modular-shared* NNs need to identify the underlying task structure to perform effectively. We measure how well these NNs capture the true task structure using minimum graph edit distance (Abu-Aisheh et al., 2015), comparing the learned inter-module connectivity to the ground truth function graph.

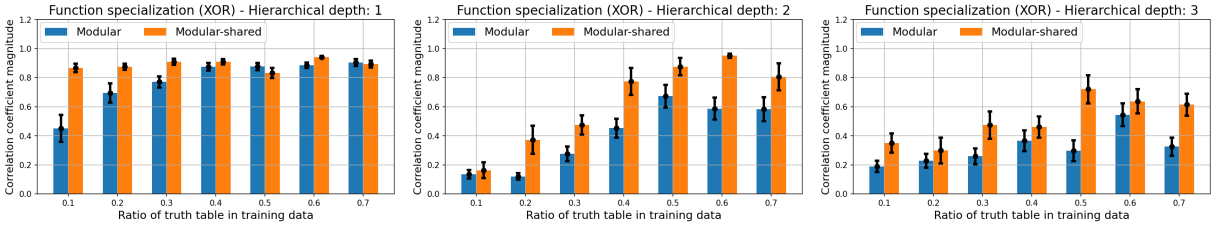

Figure 6: Magnitude of the correlation coefficient between NN module output and the XOR truth table output. Larger values indicate greater functional specialization.

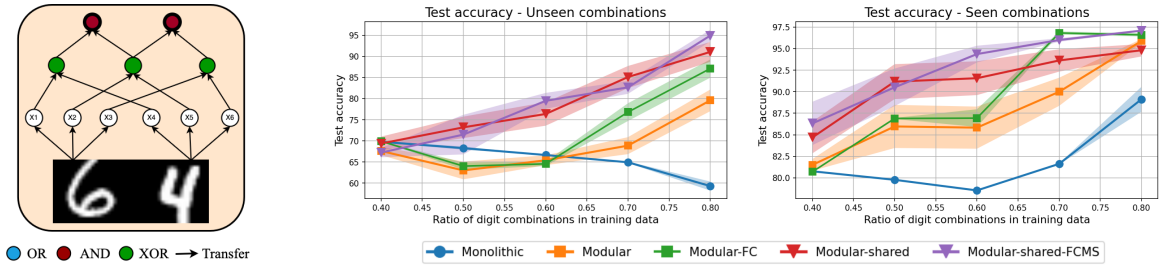

(a) MNIST task

(b) Generalization performance of various NN architectures.

Figure 7: Hierarchically modular task based on MNIST and generalization performance of various NN architectures on unseen digit combinations and seen digit combinations.

The learned connectivity is represented as a graph with NN input units, output units, and all modules as nodes. The input and output nodes must match, while modules can align with any gate node at the same hierarchical level, ensuring permutation invariance. Figure 5 shows that *modular-shared* NNs consistently achieve lower graph edit distances compared to *modular* NNs, indicating a closer match to the ground truth. Notably, the graph edit distance is zero when both *modular* and *modular-shared* NNs achieve 100% train and test accuracy.

Learning the Underlying Sub-Function: The superior generalization of *modular-shared* NNs, particularly with lower truth table ratios, suggests an advantage due to module reuse across multiple locations, enabling modules to learn sub-functions more effectively with fewer samples. To quantify functional specialization, we use a metric based on Pearson's correlation coefficient between module outputs and truth table outputs for a specific sub-function.

Let X represent all truth table rows for a specific sub-function. We collect the corresponding module outputs and calculate the correlation coefficient ρ between these outputs and the ground truth. A higher magnitude of ρ indicates greater alignment between the module's function and the ground truth sub-function.

Figure 6 shows the correlation coefficients for the XOR sub-function in the first hierarchical level of all three functions. Modules in *modular-shared* NNs exhibit consistently higher correlation with the ground truth compared to *modular* NNs, with ρ values closely aligning with generalization performance.

4 Visual Modular Task Based on MNIST

We present results for a modular task constructed using the MNIST handwritten digits dataset, as shown in Figure 7a. In this task, two MNIST images, each selected from digits between 0 and 7, serve as input. These images are classified into their corresponding 3-bit binary representations, which are then concatenated and passed to a Boolean task. The NNs must first classify each image independently before performing additional operations.

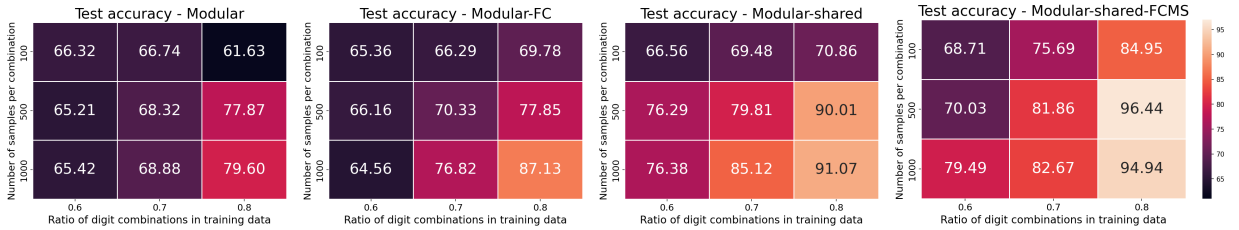

Figure 8: Generalization performance of different NNs trained on the hierarchically modular MNIST task, evaluated across varying proportions of digit combinations used for training and different numbers of samples per combination. Plots show results for: a. *modular* NN, b. *modular-FC* NN, c. *modular-shared* NN, and d. *modular-shared-FCMS* NN.

We vary the ratio of unique digit combinations used for training. For each training size, a random subset of all possible digit combinations is chosen, with the remaining combinations evenly divided between test and validation sets. We also present results on a test set constructed using seen digit combinations but with unseen digit images. Each training combination contains 1000 samples, while the test and validation sets contain 100 samples per combination. We also examine the effect of different numbers of samples per combination for training.

We adapted the NNs for handling image inputs: in *modular* NNs, the first hierarchical level contains MLP modules designed for image processing, with 784 input units, two hidden layers (128 and 64 units), and 3 output units. Each module processes one of the two images, and the outputs are concatenated and passed to higher levels, where modules learn Boolean functions, similar to previous experiments. In *modular-shared* NNs, two sets of shared modules are employed—one set for image processing and another for Boolean functions. The first layer contains two slots, each selecting an image-processing module from the shared pool, with outputs concatenated and passed to higher layers that use shared Boolean modules. For monolithic NNs, the input size was increased to 784×2, and the architecture was adjusted to match the depth and number of hidden units in the *modular* NN. All models were trained for 200 epochs using the Adam optimizer, with three dataset splits and three different seeds for each split (see Appendix Section A for additional details).

Generalization on Unseen Digit Combinations: Figure 7b shows the generalization performance on both unseen and seen digit combinations. At a training size of 0.4, all NNs show random test accuracy. As the training size increases, *modular*, *modular-shared*, *modular-FC*, and *modular-shared-FCMS* NNs start to generalize at different rates, while monolithic NNs do not improve and their test accuracy declines. This decrease may be due to over-fitting on seen digit combinations given that, for larger training sizes, the test accuracy of monolithic NNs on seen digit combinations improves.

The ability to generalize to unseen combinations, known as combinatorial generalization, is a persistent challenge for monolithic NNs (Keysers et al., 2019; Csordás et al., 2020). However, for Boolean tasks, monolithic NNs demonstrated the capacity to capture the underlying function and generalize as well as *modular* NNs, suggesting that simpler tasks and higher data availability can enable generalization.

Modular-shared NNs outperform monolithic, *modular*, and *modular-FC* NNs for the MNIST-based task. Additionally, *modular* and *modular-shared* NNs closely track their fixed-connectivity counterparts (*modular-FC* and *modular-shared-FCMS*, respectively), with small accuracy differences. This may be attributed to the large sample size used in the task, which facilitates better generalization.

Figure 8 presents the generalization performance of various NNs across different sample sizes per digit combination. We observe that *modular-shared-FCMS* NNs consistently outperform other architectures when the sample size is reduced to 500 and 100, supporting our previous hypothesis. Additionally, *modular-shared* NNs exhibit superior generalization compared to *modular* and *modular-FC* NNs, emphasizing the advantage of module reusability in low-sample training scenarios.

Generalization on Seen Digit Combinations: Figure 7b illustrates the generalization performance on seen digit combinations. It is noteworthy that the validation set contains combinations distinct from both the training and test sets. The overall trends observed in previous results are consistent here. With

larger training sizes, monolithic NNs demonstrate effective generalization. Notably, the *modular-FC* and *modular-shared-FCMS* architectures outperform the *modular* and *modular-shared* NNs at larger training sizes, emphasizing the advantage of leveraging predefined connectivity to facilitate learning of the complete task, encompassing both seen and unseen combinations.

Training Efficiency: The FLOPs required by various NNs during training are shown in Figure 9. Monolithic dense NNs show lower training costs at smaller training sizes, primarily because they reach their highest validation accuracy after just one epoch for sizes 0.4, 0.5, and 0.6, indicating limited learning. While monolithic NNs match the training efficiency of other NNs at larger training sizes, they still fall short in generalization performance.

For larger training sizes, *modular* and *modular-shared* NNs achieve training efficiencies comparable to those of *modular-FC* and *modular-shared-FCMS* NNs. This suggests that when sufficient data is available, the advantage of knowing the underlying sub-function organization has a limited impact on training efficiency. However, in data-scarce scenarios, this structural knowledge becomes crucial for effective training and generalization.

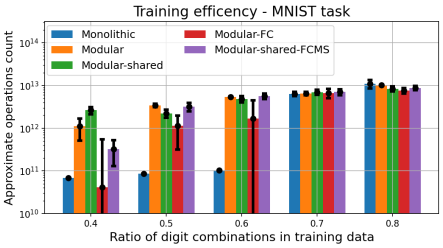

Figure 9: FLOPs required to train various NNs on the hierarchically modular MNIST task.

Learning the Sub-Function Organization: Similar to the Boolean function graphs, we compare the learned inter-module connectivity in *modular* and *modular-shared* NNs for the MNIST-based task by computing the minimum graph edit distance between the learned connectivity and the ground truth function graph.

The task graph includes two input nodes (one for each image), each connected to three of six intermediate nodes in the first hierarchical level, corresponding to six output bits (three per image). These nodes are then connected to the rest of the Boolean function graph. To construct the learned connectivity graph, we represent each image module as three nodes, with incoming connections from the input nodes and outgoing connections to subsequent modules. Our results (Figure 10) indicate that *modular-shared* NNs more accurately capture the underlying connectivity compared to *modular* NNs.

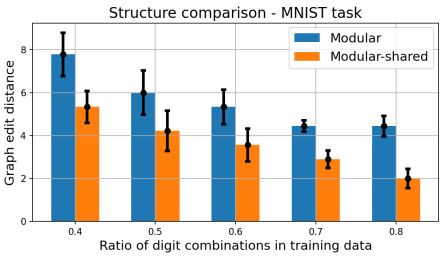

Figure 10: Minimum graph edit distance between learned connectivity and ground truth task connectivity

Learning the Underlying Sub-Function: Next, we evaluate the functional specialization of modules in both *modular* and *modular-shared* NNs, focusing on the image classification modules. We assess specialization using the magnitude of the Pearson correlation coefficient. Each module produces three outputs, while the ground truth classes are represented as 3-bit vectors.

We determine the optimal permutation of the output units by maximizing the correlation coefficient and report the highest value achieved. Our results, shown in Figure 11, reveal that modules in *modular-shared* NNs exhibit a greater degree of functional specialization compared to those in *modular* NNs, reinforcing the advantage of module reusability.

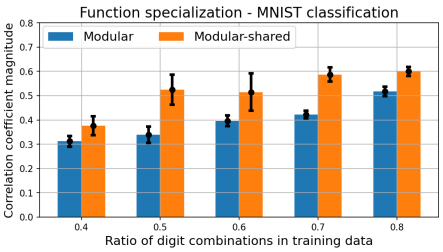

Figure 11: Function specialization in image modules for *modular* and *modular-shared* NNs.

5 Conclusion

This work explored how varying degrees of structural knowledge about a task's hierarchical modularity impacts NN generalization performance and training efficiency. Through experiments involving Boolean functions and a hierarchically modular MNIST task, we showed that NNs incorporating modularity and

module reusability significantly outperform monolithic and sparse networks, particularly in data-limited scenarios. The improved performance stems from the ability of these NNs to exploit task structure effectively by learning both the specific sub-functions and their organization. Our findings emphasize the importance of explicitly incorporating task structure through modularity and module reusability into NNs, indicating a promising direction for scalable and efficient learning systems.

Our study is deliberately grounded in tasks with fully known, static modular structure, enabling isolation of architectural factors such as sparsity, modularity, and module reuse. Extending these insights to more complex, real-world domains—where task structure is implicit and must be inferred—remains an important direction for future work. Future work could further explore the theoretical foundations of task learnability with respect to function graph complexity and the degree of encoded structural knowledge. Additionally, applying modular architectures in transfer learning settings and investigating how structural similarity between pretraining and target tasks influences efficiency and generalization may offer valuable directions for scalable learning systems.

Appendix Summary

The appendix provides additional details, results and experiments supporting the claims presented in the main part of the paper.

- **Technical Details:** Appendix A provides implementation details for the datasets and NN architectures, along with a link to the codebase. Appendix B describes how training operation counts are computed for each architecture.
- **Hierarchically Modular NN Ablations:** In the main results, *modular* and *modular-FC* architectures use the same number of modules as gate nodes in each level of the function graph. Likewise, *modular-shared* and *modular-shared-FCMS* match the number of slots to gate nodes, and the number of shared modules to distinct gates. Appendix C shows that varying the number of modules or slots has minimal impact on performance. All module MLPs share a fixed architecture, and the number of inputs to each module is kept constant. Appendix D further shows that generalization is robust to changes in module input dimensionality.
- **Multi-task Learning:** Appendix E explores a multi-task learning setup where NNs are trained to solve multiple Boolean functions simultaneously. This enables task-conditioned modularity, allowing NNs to adapt connectivity and module usage based on a task identifier. Hierarchically modular NNs naturally benefit from this flexibility. Our results show that in the multi-task case, both *modular* and *modular-shared* NNs outperform dense monolithic NNs.
- **Design Choices and Hyperparameters:** Appendix F presents additional experiments supporting the architectural and training choices for *modular* and *modular-shared* NNs. These include comparisons of input selection strategies in *modular* NNs, and module selection mechanisms in *modular-shared* NNs. We also examine the effect of different learning rates for structural and functional parameters, finding that higher learning rates for structural parameters tend to improve generalization.
- **Additional Results:** Appendix G provides supplementary visualizations offering alternative perspectives on generalization performance and training efficiency across the different architectures.

References

Zeina Abu-Aisheh, Romain Raveaux, Jean-Yves Ramel, and Patrick Martineau. An exact graph edit distance algorithm for solving pattern recognition problems. In *4th International Conference on Pattern Recognition Applications and Methods 2015*, 2015.

Jacob Andreas, Marcus Rohrbach, Trevor Darrell, and Dan Klein. Neural module networks. In *Proceedings of the IEEE conference on computer vision and pattern recognition*, pp. 39–48, 2016.

Dzmitry Bahdanau, Shikhar Murty, Michael Noukhovitch, Thien Huu Nguyen, Harm de Vries, and Aaron Courville. Systematic generalization: what is required and can it be learned? *arXiv preprint arXiv:1811.12889*, 2018.

Dzmitry Bahdanau, Harm de Vries, Timothy J O'Donnell, Shikhar Murty, Philippe Beaudoin, Yoshua Bengio, and Aaron Courville. Closure: Assessing systematic generalization of clevr models. *arXiv preprint arXiv:1912.05783*, 2019.

Yoshua Bengio, Nicholas Léonard, and Aaron Courville. Estimating or propagating gradients through stochastic neurons for conditional computation. *arXiv preprint arXiv:1308.3432*, 2013.

Michael B Chang, Abhishek Gupta, Sergey Levine, and Thomas L Griffiths. Automatically composing representation transformations as a means for generalization. *arXiv preprint arXiv:1807.04640*, 2018.

Zitian Chen, Yikang Shen, Mingyu Ding, Zhenfang Chen, Hengshuang Zhao, Erik G Learned-Miller, and Chuang Gan. Mod-squad: Designing mixtures of experts as modular multi-task learners. In *Proceedings of the IEEE/CVF Conference on Computer Vision and Pattern Recognition*, pp. 11828–11837, 2023.

Róbert Csordás, Sjoerd van Steenkiste, and Jürgen Schmidhuber. Are neural nets modular? inspecting functional modularity through differentiable weight masks. *arXiv preprint arXiv:2010.02066*, 2020.

Vanessa D'Amario, Tomotake Sasaki, and Xavier Boix. How modular should neural module networks be for systematic generalization? *Advances in Neural Information Processing Systems*, 34:23374–23385, 2021.

Chrisantha Fernando, Dylan Banarse, Charles Blundell, Yori Zwols, David Ha, Andrei A Rusu, Alexander Pritzel, and Daan Wierstra. Pathnet: Evolution channels gradient descent in super neural networks. *arXiv preprint arXiv:1701.08734*, 2017.

Xavier Glorot and Yoshua Bengio. Understanding the difficulty of training deep feedforward neural networks. In *Proceedings of the thirteenth international conference on artificial intelligence and statistics*, pp. 249–256, 2010.

Anirudh Goyal, Alex Lamb, Jordan Hoffmann, Shagun Sodhani, Sergey Levine, Yoshua Bengio, and Bernhard Schölkopf. Recurrent independent mechanisms. *arXiv preprint arXiv:1909.10893*, 2019.

Anirudh Goyal, Aniket Rajiv Didolkar, Nan Rosemary Ke, Charles Blundell, Philippe Beaudoin, Nicolas Heess, Michael Curtis Mozer, and Yoshua Bengio. Neural production systems. In *Advances in Neural Information Processing Systems*, 2021.

Hussein Hazimeh, Zhe Zhao, Aakanksha Chowdhery, Maheswaran Sathiamoorthy, Yihua Chen, Rahul Mazumder, Lichan Hong, and Ed Chi. Dselect-k: Differentiable selection in the mixture of experts with applications to multi-task learning. *Advances in Neural Information Processing Systems*, 34:29335–29347, 2021.

Ronghang Hu, Jacob Andreas, Marcus Rohrbach, Trevor Darrell, and Kate Saenko. Learning to reason: End-to-end module networks for visual question answering. In *Proceedings of the IEEE international conference on computer vision*, pp. 804–813, 2017.

Dieuwke Hupkes, Verna Dankers, Mathijs Mul, and Elia Bruni. Compositionality decomposed: how do neural networks generalise? *Journal of Artificial Intelligence Research*, 67:757–795, 2020.

Devon Jarvis, Richard Klein, Benjamin Rosman, and Andrew M Saxe. On the specialization of neural modules. *arXiv preprint arXiv:2409.14981*, 2024.

Daniel Keysers, Nathanael Schärli, Nathan Scales, Hylke Buisman, Daniel Furrer, Sergii Kashubin, Nikola Momchev, Danila Sinopalnikov, Lukasz Stafiniak, Tibor Tihon, et al. Measuring compositional generalization: A comprehensive method on realistic data. *arXiv preprint arXiv:1912.09713*, 2019.

Louis Kirsch, Julius Kunze, and David Barber. Modular networks: Learning to decompose neural computation. *Advances in neural information processing systems*, 31, 2018.

Brenden Lake and Marco Baroni. Generalization without systematicity: On the compositional skills of sequence-to-sequence recurrent networks. In *International conference on machine learning*, pp. 2873–2882. PMLR, 2018.

Samuel Lippl and Kim Stachenfeld. The impact of task structure, representational geometry, and learning mechanism on compositional generalization. In *ICLR 2024 Workshop on Representational Alignment*, 2024.

Shreyas Malakarjun Patil, Loizos Michael, and Constantine Dovrolis. Neural sculpting: Uncovering hierarchically modular task structure in neural networks through pruning and network analysis. *Advances in Neural Information Processing Systems*, 36, 2024.

Jorge A Mendez and Eric Eaton. Lifelong learning of compositional structures. *arXiv preprint arXiv:2007.07732*, 2020.

Sarthak Mittal, Yoshua Bengio, and Guillaume Lajoie. Is a modular architecture enough? *Advances in Neural Information Processing Systems*, 35:28747–28760, 2022.

Oleksiy Ostapenko, Pau Rodriguez, Massimo Caccia, and Laurent Charlin. Continual learning via local module composition. *Advances in Neural Information Processing Systems*, 34:30298–30312, 2021.

Oleksiy Ostapenko, Pau Rodriguez, Alexandre Lacoste, and Laurent Charlin. Attention for compositional modularity. In *NeurIPS'22 Workshop on All Things Attention: Bridging Different Perspectives on Attention*, 2022.

Deepak Pathak, Christopher Lu, Trevor Darrell, Phillip Isola, and Alexei A Efros. Learning to control self-assembling morphologies: a study of generalization via modularity. *Advances in Neural Information Processing Systems*, 32, 2019.

Edoardo M Ponti, Alessandro Sordoni, Yoshua Bengio, and Siva Reddy. Combining modular skills in multitask learning. *arXiv preprint arXiv:2202.13914*, 2022.

Senthil Purushwalkam, Maximilian Nickel, Abhinav Gupta, and Marc'Aurelio Ranzato. Task-driven modular networks for zero-shot compositional learning. In *Proceedings of the IEEE/CVF International Conference on Computer Vision*, pp. 3593–3602, 2019.

Nasim Rahaman, Muhammad Waleed Gondal, Shruti Joshi, Peter Gehler, Yoshua Bengio, Francesco Locatello, and Bernhard Schölkopf. Dynamic inference with neural interpreters. *Advances in Neural Information Processing Systems*, 34:10985–10998, 2021.

Clemens Rosenbaum, Tim Klinger, and Matthew Riemer. Routing networks: Adaptive selection of non-linear functions for multi-task learning. *arXiv preprint arXiv:1711.01239*, 2017.

Simon Schug, Seijin Kobayashi, Yassir Akram, Maciej Wołczyk, Alexandra Proca, Johannes Von Oswald, Razvan Pascanu, João Sacramento, and Angelika Steger. Discovering modular solutions that generalize compositionally. *arXiv preprint arXiv:2312.15001*, 2023.

Noam Shazeer, Azalia Mirhoseini, Krzysztof Maziarz, Andy Davis, Quoc Le, Geoffrey Hinton, and Jeff Dean. Outrageously large neural networks: The sparsely-gated mixture-of-experts layer. *arXiv preprint arXiv:1701.06538*, 2017.

Herbert A Simon. The architecture of complexity. In *Facets of systems science*, pp. 457–476. Springer, 1991.

Alexander V Terekhov, Guglielmo Montone, and J Kevin O'Regan. Knowledge transfer in deep block-modular neural networks. In *Biomimetic and Biohybrid Systems: 4th International Conference, Living Machines 2015, Barcelona, Spain, July 28-31, 2015, Proceedings 4*, pp. 268–279. Springer, 2015.

Tom Veniat, Ludovic Denoyer, and Marc'Aurelio Ranzato. Efficient continual learning with modular networks and task-driven priors. *arXiv preprint arXiv:2012.12631*, 2020.

Jianan Wang, Eren Sezener, David Budden, Marcus Hutter, and Joel Veness. A combinatorial perspective on transfer learning. *Advances in Neural Information Processing Systems*, 33:918–929, 2020.

A Implementation and Training Details

The GitHub repository can be accessed here: `https://github.com/ShreyasMalakarjunPatil/modular-NNs`.

This section presents the implementation details for datasets, NN architectures, and training settings for all architectures.

A.1 Dataset Construction and Hyperparameter Tuning

Boolean Functions: For Boolean functions, we generate a truth table of 64 rows (6 inputs). Rows are split into training, validation, and test sets based on the specified training ratio and dataset seed. Each training size has three different splits corresponding to three different dataset seeds.

MNIST Task: The MNIST task uses pairs of digits (0-7), resulting in 64 combinations. These combinations are divided into training, validation, and test sets, similarly to the Boolean functions. For each combination, we randomly select image pairs in the MNIST training set based on the specified sample size per combination. Test sets use image pairs from the MNIST test split. Dataset splitting is performed using three different seeds. When varying the number of samples per combination, the validation and test sets remain consistent.

Training and Hyperparameter Tuning: The NNs are trained using the Adam optimizer for 1000 epochs for Boolean functions and 200 epochs for the MNIST task. The loss function is bitwise cross-entropy with Sigmoid activation. A grid search over learning rate, batch size, and weight decay is used to select optimal hyperparameters based on validation accuracy. We use seeds $\{40, 41, 42\}$ for dataset splits and $\{0, 1, 2\}$ for NN initialization and training. We independently tune the hyperparameters for each dataset split and training size by maximizing the validation accuracy, averaged over the three training seeds.

A.2 MLPs and Random Sparse MLPs

Architecture Details: We use MLPs with ReLU activations at the hidden layers, Sigmoid at the output layers, and Xavier weight initialization (Glorot & Bengio, 2010). Sparsity in monolithic NNs is achieved by pruning edges based on a uniform random score.

Boolean functions with depths of 1, 2, and 3 use MLPs with 1, 3, and 5 hidden layers (36 units each). The MNIST-based task uses MLPs with 784×2 input units, 2 output units, and 6 hidden layers with $256, 128, 64, 36, 36, 36$ units.

Hyperparameter Sets: For Boolean functions, we use learning rates $\{0.1, 0.01, 0.001\}$, batch sizes $\{4, 64\}$, and weight decay $\{0.001, 0.0001\}$. For MNIST, we test learning rates $\{0.01, 0.001\}$, batch sizes $\{128, 256, 512\}$, and weight decay $\{0.001, 0.0001\}$.

A.3 Hierarchically Modular NNs

Overall Architecture: The architecture has L hierarchical layers, each with M_l modules. Each module m_l^i has functional parameters (MLP) and structural parameters (input selection vector $s_l^i \in \mathbb{R}^{M_{l-1}}$). The input selection vector, initialized with values from a standard normal distribution, determines module input connectivity.

Module Input Selection: For a module m_l^i, we apply the Sigmoid function to the input selection vector s_l^i to get p_l^i, then select the top-2 values to generate one-hot encoded binary masks $b_1 \in \{0,1\}^{M_{l-1}}$ and $b_2 \in \{0,1\}^{M_{l-1}}$. These masks isolate inputs from $\boldsymbol{x}_{l-1}$ using dot products, resulting in inputs $x_1(l,i) = b_1 \odot \boldsymbol{x}_{l-1}$ and $x_2(l,i) = b_2 \odot \boldsymbol{x}_{l-1}$. The straight-through estimator is used to estimate gradients.

For image modules, the Softmax function is applied to s_l^i and one input image is selected. A binary mask, $b \in \{0,1\}^2$, is generated and applied to each pixel position across the two images.

Task	Hierarchical depth 1			Hierarchical depth 2			Hierarchical depth 3			MNIST Task		
Number of weights	F	B	U	F	B	U	F	B	U	F	B	U
Monolithic	288	288	288	2880	2880	2880	5472	5472	5472	442,744	442,744	442,744
Modular	100	100	86	232	232	206	358	358	323	220,840	220,840	217,682
Modular-shared	102	102	52	422	242	108	958	382	167	221,036	220,676	108,850
Modular-FC	72	72	72	180	180	180	288	288	288	217,652	217,652	217,652
Modular-shared-FCMS	72	72	36	180	180	72	288	288	108	217,652	217,652	108,808

Table 1: Number of weights involved in forward pass (F), backward pass (B) and gradient based update (U) of various NNs for different tasks.

Forward Pass: Each module's input is processed by its MLP, and outputs are concatenated before passing to the next layer. This is repeated until the final layer, where outputs are selected from the last set of modules using input selection vectors.

Module MLP Architectures: For Boolean sub-functions, module MLPs have 2 input units, 1 output unit, and a hidden layer with 12 units. For MNIST, module MLPs have 784 input units, 3 output units, and 2 hidden layers (128 and 64 units). Xavier initialization is used for weights.

Hyperparameter Sets: Hyperparameters include learning rates $\{0.1, 0.01\}$, batch sizes $\{4, 64\}$, and weight decay $\{0.001, 0.0001\}$ for Boolean functions. MNIST uses learning rates $\{0.01, 0.001\}$, batch sizes $\{128, 256, 512\}$, and weight decay $\{0.001, 0.0001\}$. Structural and functional parameters use separate learning rates, and activation function temperature (τ) for input selection vectors is also tuned ($\{1.0, 2.0, 5.0\}$).

The learning rate values tested here for Boolean functions is a subset of the one used for monolithic NNs while the batch size and weight decay values are the same. The learning rates and temperatures used here are selected from a broader range of values based on results in Appendix F.1 and F.2.

Fixed Connectivity: In fixed inter-module connectivity, input selection vectors are fixed, and gradients are not computed for them. A single learning rate is used for functional parameters, and the hyper-parameter sets tested are consistent with the setup for monolithic NNs.

A.4 Hierarchically Modular NNs with Shared Modules

Overall Architecture: The architecture consists of L layers with M_l slots, filled by modules from a shared pool of M modules. Each slot has an input selection vector ($\boldsymbol{s}_l^i$) and a module selection vector ($\boldsymbol{v}_l^i$). Both vectors are initialized randomly with samples from the standard normal distribution.

Input and Module Selection: Input selection follows the same procedure as for standard hierarchically modular NNs. For module selection, the Softmax function is applied to $\boldsymbol{v}_l^i$ to select a module from the pool and a binary mask, $b \in \{0, 1\}^M$ is constructed. The inputs to the slots are passed through all M modules, and the slot output is computed using a dot product between the module outputs and the binary mask. The straight-through estimator is used for gradient calculation. For image slots, the module selection mask is applied independently at each module output position.

Forward Pass: Each slot processes inputs using a selected module, and the outputs are concatenated and passed to subsequent layers. The module MLP architecture, training, and hyperparameters are consistent with those used for hierarchically modular NNs.

Fixed Connectivity and Module Selection: In this variant, both input and module selection vectors are fixed, with no gradients computed. The same hyperparameters are used as for monolithic NNs.

B Training Efficiency Details

This section describes the methodology used to calculate the number of floating-point operations (FLOPs) required during training across various NN architectures. In practice, GPU hardware performs dense matrix multiplications, even when the weight matrix is sparse. However, in the hierarchically modular architectures, computational savings arise from modules that are small, independent MLPs—each with significantly fewer parameters than their monolithic counterparts. These smaller MLPs naturally lead to reduced FLOP counts, irrespective of GPU implementation details. In the case of sparse monolithic NNs, we report FLOP reductions

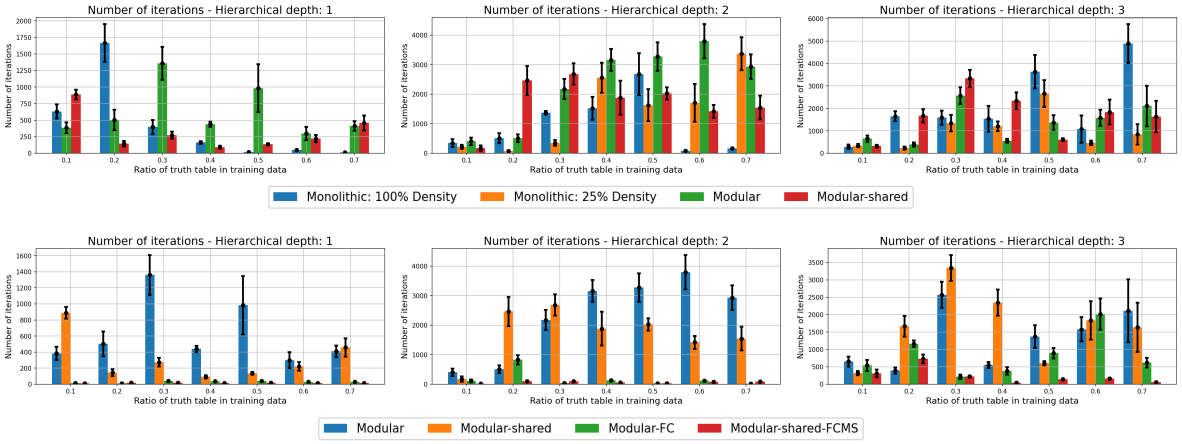

Figure 12: Number of weight updates (training iterations) for various NNs to reach peak validation accuracy on different Boolean functions as compared to the ratio of truth table available.

based on parameter sparsity; however, these do not translate to actual computational gains on GPUs due to the lack of native support for sparse matrix operations.

The three main factors determining the FLOP count are: the number of samples or training size, the number of parameters, and the number of training iterations (or weight updates) needed to reach the highest validation accuracy (i.e., early stopping). Figures 12 and 13 present the number of training iterations required by different NN architectures, while Table 1 summarizes the weights involved in forward, backward, and gradient update processes for various tasks.

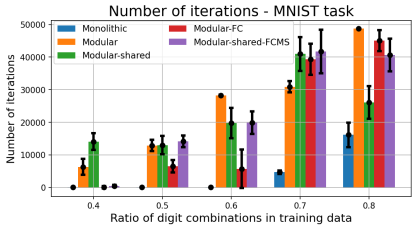

Figure 13: Number of weight updates (training iterations) for various NNs to reach peak validation accuracy on the MNIST-based task.

In each training iteration, given a batch size b, there are b forward passes, b backward passes, and one weight update. For a dataset of size D over one epoch, this results in D forward passes, D backward passes, and $\lfloor D/b \rfloor + 1$ weight updates. The total FLOP count is computed by multiplying the number of epochs by the operations performed during all forward passes, backward passes, and weight updates per epoch. FLOPs related to activation functions and biases are excluded from this calculation.

Monolithic NNs: Let W be the number of weights in a dense, monolithic NN. The FLOP count for a single forward pass through the linear layers is $2 \times W$. For the backward pass, this count is $4 \times W$. Weight updates using the Adam optimizer require $18 \times W$ operations.

For random sparse monolithic NNs, the number of weights is scaled according to the network's density, and FLOP calculations follow the same approach as for dense NNs.

Hierarchically Modular NNs: In hierarchically modular NNs, the total FLOP count includes both operations from the forward pass through each module and those from the module input selection mechanism. For Boolean function modules, input selection involves two dot products; for image modules, it involves 784 dot products, effectively introducing additional units (2 for Boolean modules and 784 for image modules) to process the full output of the previous layer. The parameters for input selection vectors are also considered in weight updates, and the FLOP counts for the forward and backward passes incorporate $2\times$ or $784\times$ the parameters for the input selection vectors for Boolean and image processing modules, respectively. The rest of the calculations follow the previously described procedures.

In the variant with fixed inter-module connectivity, we do not include any FLOPs related to input selection and only consider the weights within the module MLPs for the FLOP calculations.

Hierarchically Modular NNs with Shared Modules: For hierarchically modular NNs with shared modules, each slot processes its specific inputs through all shared modules. A dot product is performed between the activated module selection vector and the outputs of all modules, increasing the number of parameters involved in the forward pass.

Let W_m represent the number of weights in each module MLP, N_s be the number of slots, and M the number of shared modules. The number of weights used in the forward pass is $W_m \times N_s \times M$. In the backward pass, the number of active weights is reduced to $W_m \times N_s$ because the module selection mask is binary, leading to zero gradients for unselected modules in each slot.

For accounting for FLOPs associated with input selection vectors during forward and backward pass we utilize the same procedure as described for hierarchically modular NN. Module selection involves a dot product between the outputs of all modules and the module selection mask, effectively adding units (1 for Boolean modules and 3 for image modules) at the top of each slot. The forward and backward pass incorporates $1\times$ or $3\times$ the parameters for the module selection vectors for Boolean modules and image processing modules respectively.

Finally, for weight updates using the Adam optimizer, we account for the parameters in the input selection vectors, module selection vectors, and all shared modules.

The number of weights involved in the forward pass, backward pass, and optimizer updates is scaled according to the respective operations (refer to details for monolithic NNs). The total FLOP count is then obtained by multiplying these operations by the number of training epochs.

For the variant with fixed inter-module connectivity and module selection, FLOPs related to input and module selection are excluded, and only the weights in the module MLPs are considered. During the forward and backward passes, the number of active modules equals the number of slots, while weight updates are applied only to the shared modules.

C Experiments with Arbitrary Modular Architectures

In this paper, we initialize *modular* NNs with a number of modules that matches the function graph at each hierarchical level. For *modular-shared* NNs, we use the same number of slots per hierarchical level as in the function graph, while the number of shared modules corresponds to the number of distinct gates in the function graph. However, an important question arises: how effective are these hierarchically modular architectures when such structural information is unknown, and an arbitrary number of modules or slots are initialized?

In this section, we present results for scenarios where we vary the number of modules/slots at each hierarchical level, as well as the number of shared modules for the *modular-shared* architecture. These experiments provide insights into the flexibility and robustness of hierarchically modular NNs under less structured initialization conditions. We consider the Boolean function shown in Figure 14, and the hierarchically modular NNs are trained following the methodology outlined in Section A.

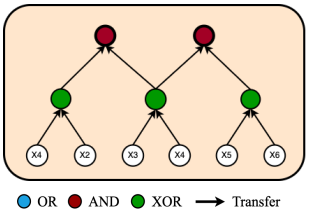

Figure 14: Function graph

C.1 Hierarchically Modular NNs

In the case of *modular* NNs, as depicted in the function graph in Figure 14, the NN requires three modules at the first hierarchical level and two modules at the second. To evaluate the flexibility of the module count, we experiment with three additional architectures, where each hierarchical level is assigned M modules, varying M from 3 to 9.

Each architecture is trained independently using different training size ratios of the truth table, as described in Section A. The resulting training and test accuracy values are shown in Figure 15.

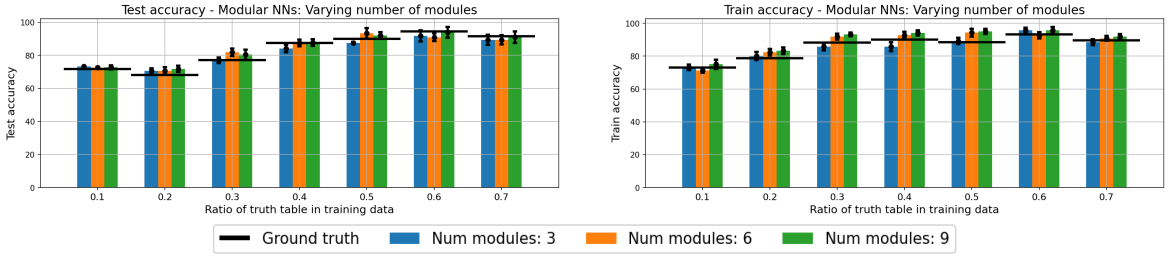

Figure 15: Train and test accuracy as compared to the number of modules defined in each layer of the *modular* NN. The black lines represent the accuracy for the model with ground truth number of modules in each layer.

Interestingly, the performance across these architectures remains comparable to the NN that uses the ground truth number of modules per hierarchical level. Furthermore, our analysis does not show a clear trend where increasing or decreasing the number of modules consistently improves performance, suggesting that the architecture is robust to variations in module count.

C.2 Hierarchically Modular NNs with Shared Modules

For *modular-shared* NNs, we explore architectural variations along two dimensions, organized in a grid. The first dimension is the number of slots per hierarchical level, ranging from $\{3, 6, 9\}$, and the second is the total number of shared modules, varying across $\{2, 4, 8\}$. This setup results in nine distinct architectures, each defined by a unique combination of slot and shared module counts.

Each architecture is trained independently using different splits of the truth table, with varying fractions allocated for training. The results are presented in Figure 16, with plots segmented by the ratio of the truth table used for training. The horizontal black line in the figure indicates the performance of the architecture configured with the ground truth number of slots and shared modules.

Consistent with our previous analysis, we observe that these architectures perform comparably to the ground truth setup. However, *modular-shared* NNs with a larger number of slots outperform the ground truth configuration at smaller training sizes. Additionally, *modular-shared* NNs with more shared modules than slots (e.g., three slots per hierarchical level and two shared modules) exhibit reduced generalization performance at larger training sizes, suggesting that an imbalance between slots and shared modules may limit effective module reuse.

D Effect of module input size on generalization performance

Previous research has demonstrated that constraining module input dimensions or introducing input bottlenecks enhances functional specialization, thereby improving generalization performance. The underlying intuition is that by promoting sparsity—considering only a subset of outputs from preceding layers—the modules more effectively capture the sub-function structure they are designed to learn. In our experiments, we align the number of module inputs with the dimensions of their corresponding sub-functions: two inputs for Boolean modules and one input for image modules. This section presents the experiment and results obtained by varying the input dimensions of the modules in *modular* and *modular-shared* NNs. We consider the Boolean function shown in Figure 14, and the hierarchically modular NNs are trained following the methodology outlined in Section A.

***Modular* NNs:** We evaluate *modular* NNs configured with 6 and 9 modules at each hierarchical level, allowing the module input dimensions to vary between 2, 4, and 6. If the number of modules were reduced to fewer than 3 or 2, the maximum possible input dimensions for modules at higher hierarchical levels would be constrained by this reduced number.

When the module input dimension matches the number of outputs from the previous layer, we explore two approaches: 1. Feeding the entire output directly into the modules without leveraging the module's input

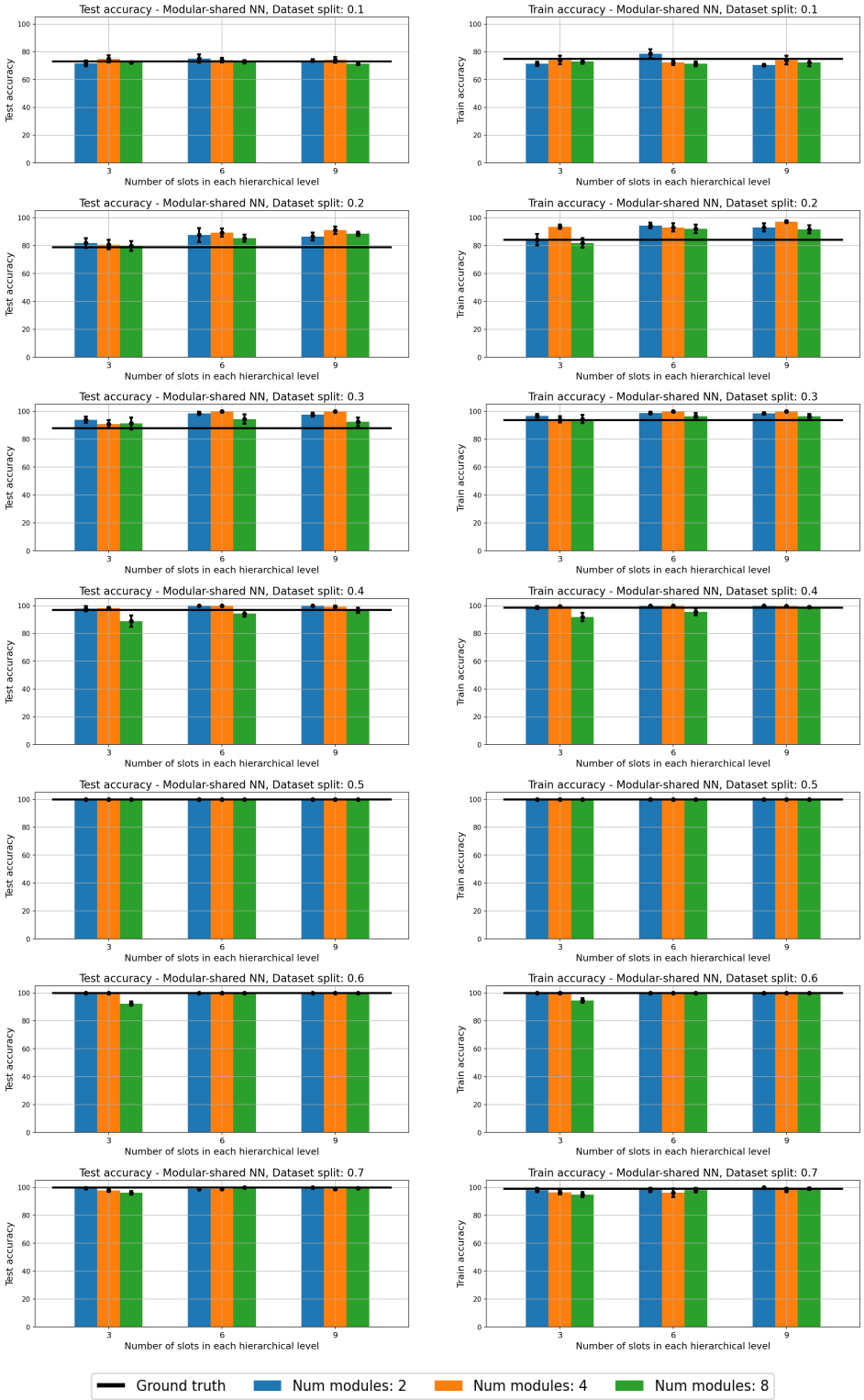

Figure 16: Train and test accuracy as compared to the number of slots defined in each layer and the number of modules in the *modular-shared* NN. The black curve represents the accuracy for the model with ground truth number of slots in each layer and the ground truth number of shared modules.

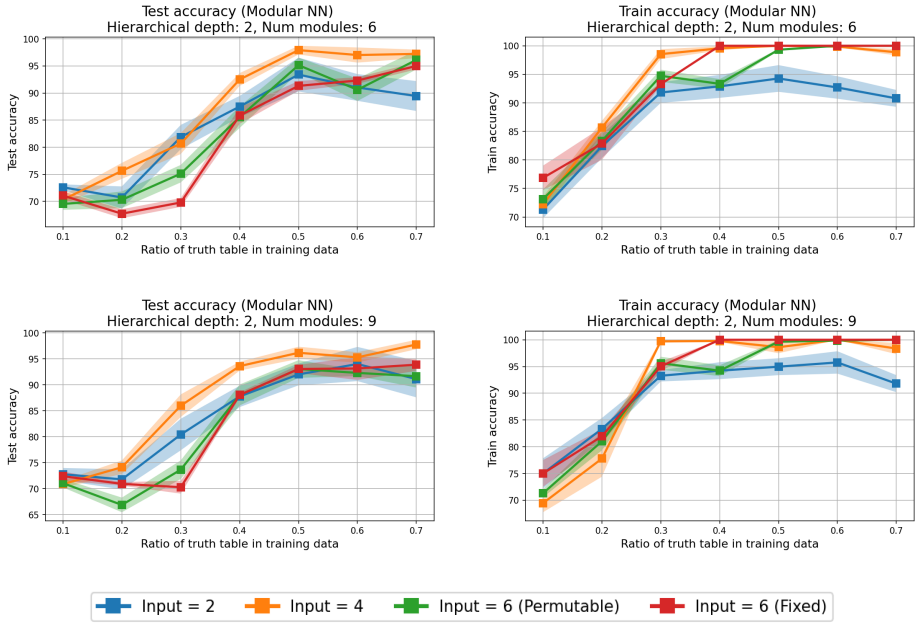

Figure 17: Train and test accuracy as compared to the number of module inputs in the *modular* NN.

selection vectors; 2. Utilizing input selection vectors to rank and reorder inputs. Figure 17 presents the training and testing accuracy for modular NNs with varying numbers of modules and input dimensions.

Our findings indicate that a module input dimension of 4 yields the highest training and testing accuracy. However, configurations with 2 inputs (aligned with the sub-functions in the function graph) or 6 inputs (matching the overall input dimension of the NN) perform comparably at higher training sizes. Notably, when the input dimension is set to 2, performance slightly surpasses that of 6 at lower training sizes. Conversely, modules with 6 inputs achieve better training accuracy than those with 2 inputs, indicating that larger input dimensions may facilitate over-fitting.

This result indicates that knowledge of the exact module input size (ground truth of 2) does not significantly impact the generalization performance of *modular* NNs. However, introducing some form of input sparsity appears to provide a slight improvement in generalization performance, likely by promoting better specialization and alignment with the underlying task structure.

***Modular-shared* NNs:** For *modular-shared* NNs, we experimented with architectures comprising 6 and 9 slots at each hierarchical level and module input dimensions of 2, 4, and 6. The corresponding results are illustrated in Figure 18.

The results show that module input sizes of 2 and 4 yield significantly higher test accuracy compared to an input size of 6 when slots are not allowed to reorder or permute their inputs. However, when slots are permitted to perform input permutations, the advantage of input sparsity (input sizes of 2 and 4) diminishes, with only a slight margin of improved performance over input size 6.

Effect of Permutations with Full Module Inputs: A key observation is that when a module's input dimension equals the full output of the previous layer (i.e., no input sparsity), allowing modules to permute their inputs significantly improves performance in *modular-shared* NNs. For example, consider a module with more than two input units tasked with learning the XOR function for two inputs. If the module learns the XOR gate for two specific input positions, it can only be reused in slots requiring XOR computation for those same positions. By enabling input permutation, the module generalizes and can be reused across any slot where XOR functionality is needed, regardless of input order. This enhanced flexibility improves module reuse and contributes to better generalization.

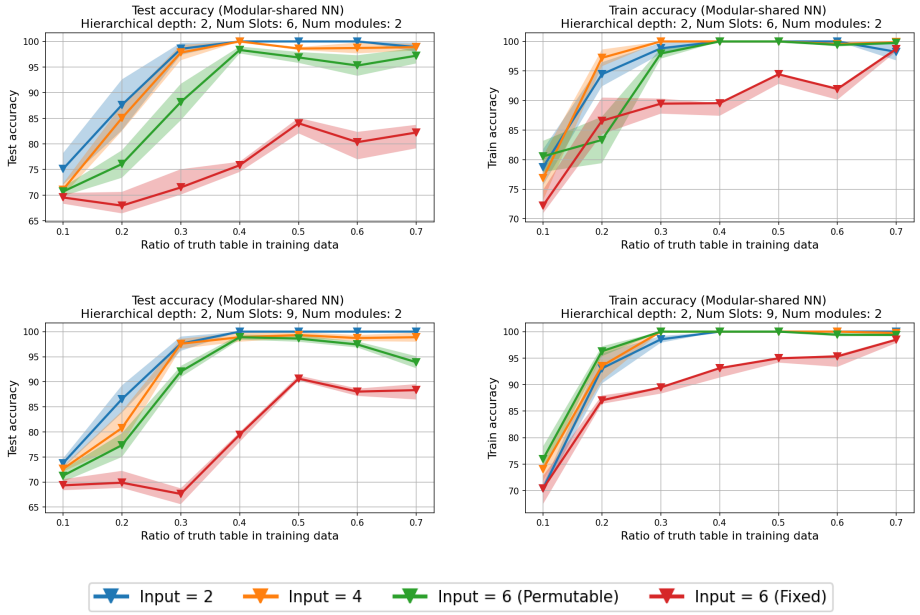

Figure 18: Train and test accuracy as compared to the number of module or slot inputs in the *modular-shared* NN.

Overall, the results indicate that knowledge of the exact module input size (ground truth of 2) does not significantly affect the generalization performance of *modular-shared* NNs when input reordering is allowed, facilitating effective module reuse. Nevertheless, introducing input sparsity (e.g., input dimensions of 2 or 4) provides a slight improvement in generalization, likely due to better functional specialization and alignment with the task's modular structure. These findings suggest that the superior generalization performance of *modular-shared* NNs is primarily driven by module reuse, with input sparsity acting as a complementary factor that refines specialization.

E Multi-task learning

We extend our experimental setup to explore multi-task learning scenarios where each neural network (NN) architecture is trained to perform multiple Boolean functions simultaneously. This allows us to evaluate task-conditioned modularity by enabling networks to adjust connectivity and module selection based on a task identifier provided with each input sample.

E.1 Experimental set-up

Consider a set of n Boolean function graphs (or tasks), and their corresponding truth tables T_i, for $i \in \{1, 2, \ldots, n\}$. Consider the experimental setup described in Section 3 of the paper. For each task i, we sample an r-fraction of rows from T_i, prepend a one-hot encoded task identifier $t = i$ to each row, and combine these samples from all tasks into a unified training set. This process is repeated to create the validation and test sets.

We train three architectures:

Monolithic dense: The input dimension of the architecture is expanded to include the task identifier. The network is then trained using standard methods.

Modular: The *modular* NN is configured similarly to the single task setting, with L modular layers, containing M_l modules at layer l. Each module consists of an MLP comprising 2 input units, 12 hidden units, and 1

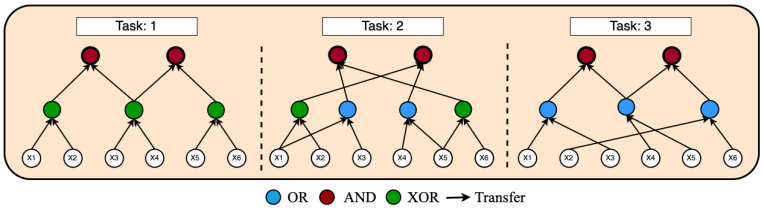

Figure 19: Function graphs used in the multi-task learning setting.

output unit, along with an input selection vector. The input selection vector is a two-dimensional matrix of size $n \times M_{l-1}$, where n represents the number of tasks.

Given the one-hot encoded task identifier associated with each input sample, the corresponding row of the input selection vector is used to determine the module's inputs or inter-module connectivity. The input selection vector can be interpreted as the weight matrix of a single linear layer that takes the task identifier as input and generates the input selection vector specific to the module and task.

Please note that the input selection vectors for all the modules are learned or trained along with all the MLP weights.

Modular-shared: Similar to the single-task *modular-shared* NN, this architecture replaces individual modules with M_l slots in each hierarchical layer l and employs a pool of M shared modules. Each slot is defined by an input selection vector of size $n \times M_{l-1}$ and a module selection vector of size $n \times M$.

For each input sample, the task identifier determines the corresponding rows of these matrices, specifying both the inter-module connectivity and the module selection at each slot. The input selection and module selection vectors for all the slots are learned or trained along with all the MLP weights.

E.2 Results

We consider the three function graphs shown in Figure 19 in the multi-task setting.

Learning two tasks (1 & 2): First, we present results for learning two of the three tasks. Here, the monolithic dense NN consists of 8 input units, 2 output units, and 3 hidden layers with 60 units in each layer. The *modular* NN comprises 5 modules in the first layer and 4 modules in the second layer. The *modular-shared* NN consists of 4 slots in the first layer, 2 slots in the second layer, and 3 shared modules.

The test accuracy and the training efficiency are presented in Figure 20(column 1). Both *modular* and *modular-shared* NNs consistently outperform the monolithic dense NN. The accuracy gap between *modular* and *modular-shared* NNs is low, likely due to the sub-function output reuse across the two tasks (e.g., 2 sub-function outputs with XOR gates are common or reused between tasks 1 and 2). *Modular* NNs with their fixed module positions, are particularly effective in capturing sub-function output reuse both across and within tasks. (See section 2 of the paper for definition)

In terms of training efficiency, both *modular* and *modular-shared* NNs require significantly fewer operations to learn the two tasks effectively. Additionally, *modular* NNs are able to match the training efficiency of *modular-shared* NNs.

Learning two tasks (1 & 3): Next, we present results for a multi-task setting where tasks 1 and 3 are learned simultaneously. The monolithic NN consists of 8 input units, 2 output units, and 3 hidden layers with 72 units in each layer. The *modular* NN consists of 6 modules in the first layer and 4 modules in the second layer. Finally, the *modular-shared* NN comprises 3 slots in the first layer, 2 slots in the second layer, and 3 shared modules.

The test accuracy and the training efficiency are presented in Figure 20(column 2). Both *modular* and *modular-shared* NNs again outperform the monolithic dense NN in terms of test accuracy and training

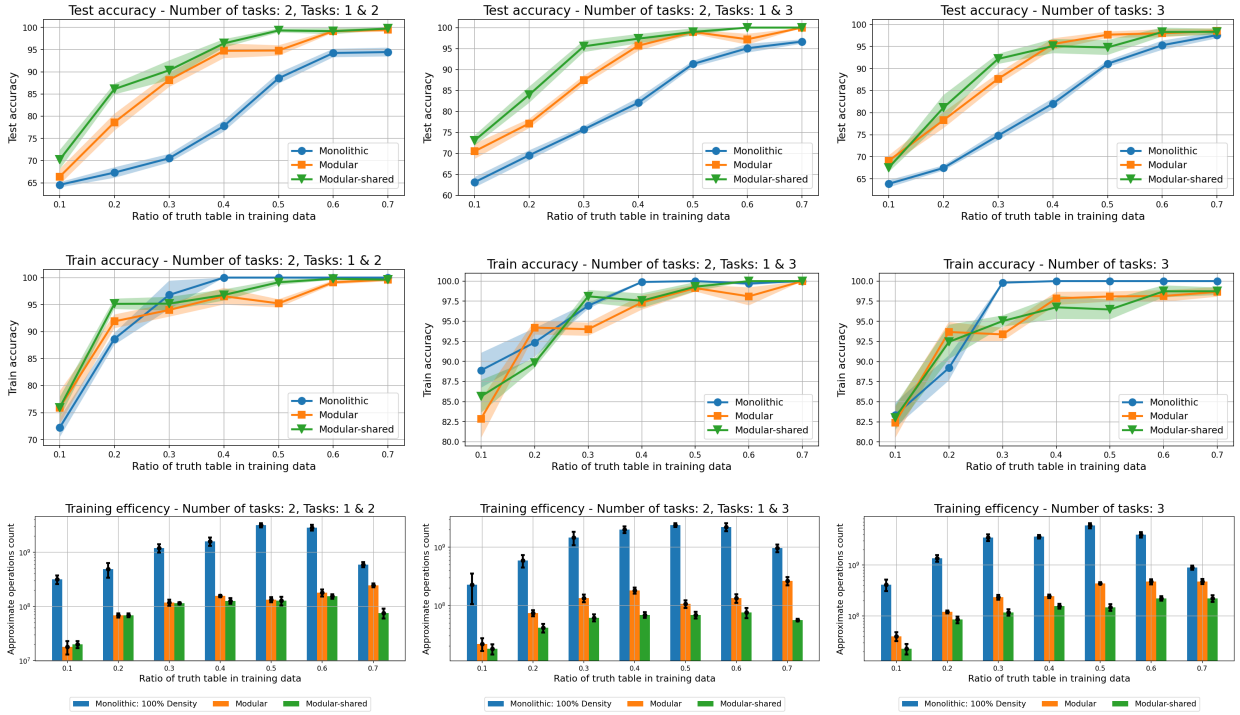

Figure 20: Test accuracy, train accuracy, and training efficiency results of various NN architectures relative to training size in the multi-task learning set-up. For each datapoint, we report the mean and combined standard error (shaded region).

efficiency. However, there is a more significant performance gap between *modular-shared* and *modular* NNs in this case. Since tasks 1 and 3 do not share sub-function outputs, the performance advantage of *modular* NNs due to common sub-function outputs is absent, leading to a larger difference in accuracy and efficiency.

Learning three tasks: Finally, we examine the multi-task setting where all three tasks are learned simultaneously. The monolithic NN has 9 input units, 2 output units, and 3 hidden layers with 72 units per layer. The *modular* NN is configured with 6 modules in both hierarchical layers. The *modular-shared* NN has 4 slots in the first layer, 2 slots in the second layer, and 3 shared modules.

Both *modular* and *modular-shared* NNs significantly outperform the monolithic dense NN in terms of generalization performance and training efficiency.

Across all training sizes, *modular* and *modular-shared* NNs show comparable test accuracy. This similarity can be attributed to the substantial amount of sub-function output reuse, which *modular* NNs can exploit due to their fixed module positions. However, *modular-shared* NNs consistently achieve superior training efficiency due to their reduced number of trainable parameters and the abundant sub-function operation reuse across the three tasks. (See section 2 of the paper for definition)

E.3 Observations and implications

The input or task-identifier-conditioned connectivity inherently favors hierarchically modular NNs, as their input-output function can adapt based on the task. In a single-task setting, where the input-output function is fixed, this advantage is less apparent. For this reason, we focused on a single-task or static setting earlier and found that modularity without module reusability does not improve generalization performance. However, in a multi-task setting where the task identifier is available, even *modular* NNs outperform monolithic dense NNs.

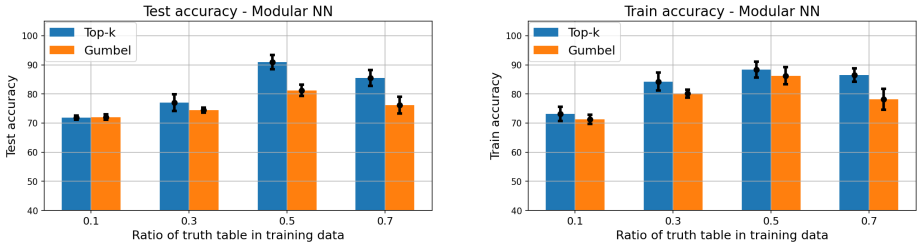

Figure 21: Train and test accuracy of *modular* NNs as compared to the ratio of the truth table used for training. The various bars indicates the addition of Gumbel noise or direct top-k for module input selection.

F Hyperparameter tuning and selection

In this section, we present additional results to support the architectural and training choices for *modular* and *modular-shared* NNs. These experiments are based on the function graph shown in Figure 14, with varying proportions of the truth table used for training. Dataset details remain consistent with those described in Section A.

We perform a grid search over learning rates for both structural and functional parameters, as well as weight decay values. Tested learning rates include $\{0.1, 0.01, 0.001\}$, while weight decay values are $\{0.001, 0.0001\}$. The batch size is set to use all available training samples in a single batch, and all networks are trained for 1000 epochs using the Adam optimizer.

F.1 Connectivity and Module Selection

In Section A, we described the process of learning structural parameters in *modular* and *modular-shared* NNs. Here, we present experiments to justify the use of the top-k operation for input connectivity and module selection in both network types.

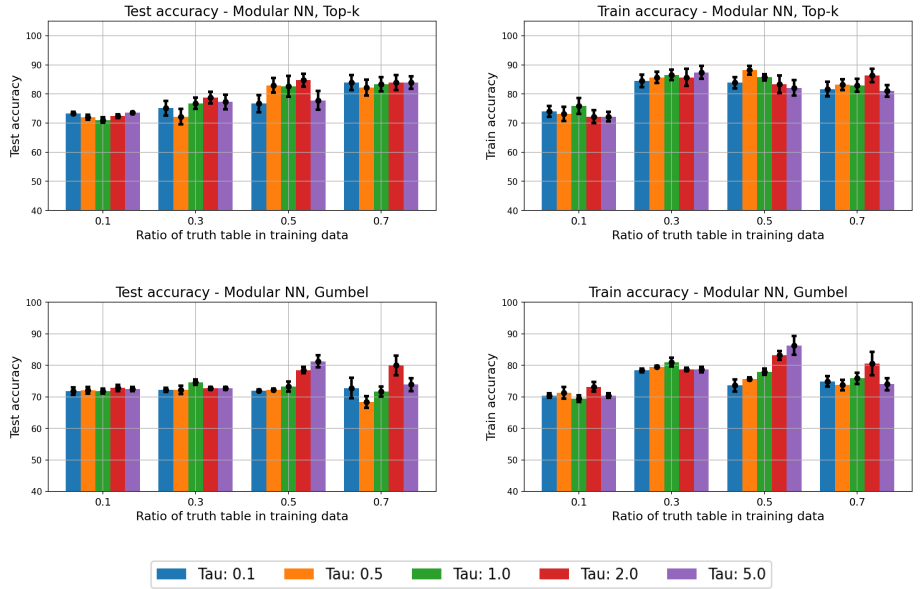

Figure 22: Train and test accuracy of *modular* NNs as compared to the temperature (tau) values used for module input selection using Gumbel noise.

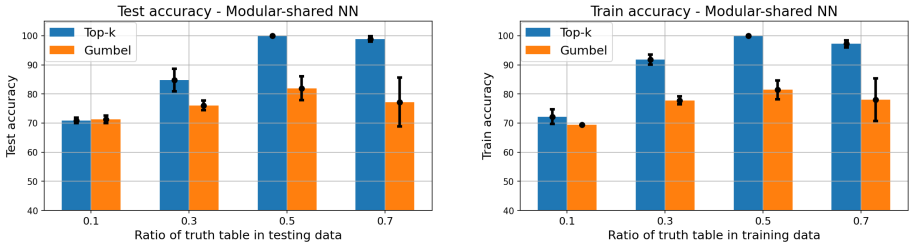

Figure 23: Train and test accuracy of *modular-shared* NNs as compared to the ratio of the truth table used for training. The various bars indicates the addition of Gumbel noise or direct top-k for module input selection.

F.1.1 Hierarchically Modular NNs

Consider the input selection vector for module m_l^i, denoted as s_l^i. The goal is to use this vector to score and select k indices along with their corresponding input values for the specific module. First, the Sigmoid function is applied to the vector, yielding $p_l^i = \sigma(s_l^i)$.

Previous training methods for hierarchically modular NNs have enhanced the exploration of different connectivity patterns by adding Gumbel-distributed noise to the input selection vector before applying a normalization function. This process allows for the effective selection of the top-k indices, promoting exploration during training.

We investigate a variant of this process where Gumbel noise is added to s_l^i before selecting the top-k indices from p_l^i. A grid search over the temperature parameter (τ) used to normalize the vector after adding Gumbel noise was also performed to identify the best configuration. This approach aims to balance exploration and exploitation, reducing the likelihood of premature convergence to suboptimal input configurations while improving learning capability.

The results are shown in Figure 21. We observe that the standard top-k selection method significantly outperforms the Gumbel noise-based variants. We also evaluate the effect of temperature on input selection performance. As depicted in Figure 22, higher temperature values yield better results. Increased temperature facilitates more uniform exploration of the input selection vector, contributing to improved learning outcomes.

F.1.2 Hierarchically Modular NNs with Shared Modules

We now present the results for the *modular-shared* architecture. Let s_l^i and v_l^i denote the input and module selection vectors for a given slot, respectively. The goal is to select k inputs and one module for each slot. The Sigmoid function is applied to s_l^i and the Softmax function is applied to v_l^i to compute the selection scores.

We compare direct top-k selection to a variant that uses Gumbel noise to enhance exploration. In this variant, Gumbel noise is added to the selection vectors before applying the normalization functions, which aims to avoid immediate convergence to a specific set of inputs or modules, promoting broader exploration during training.

Figure 23 demonstrates that Gumbel noise-based variants perform worse than the standard top-k selection. Furthermore, as shown in Figure 24, higher temperature values during input selection improve the model's performance, consistent with the findings for hierarchically modular NNs. This effect is due to increased exploration, preventing premature convergence and enhancing learning outcomes.

F.2 Learning Rate Analysis for Structural and Functional Parameters

We analyze the impact of learning rates on both the structural and functional parameters in hierarchically modular NNs. For both the *modular* and *modular-shared* architectures, we begin by fixing the learning rate combinations and then fine-tuning other hyperparameters, including weight decay and temperature values. The batch size is kept constant so that all available samples are used in each training iteration.

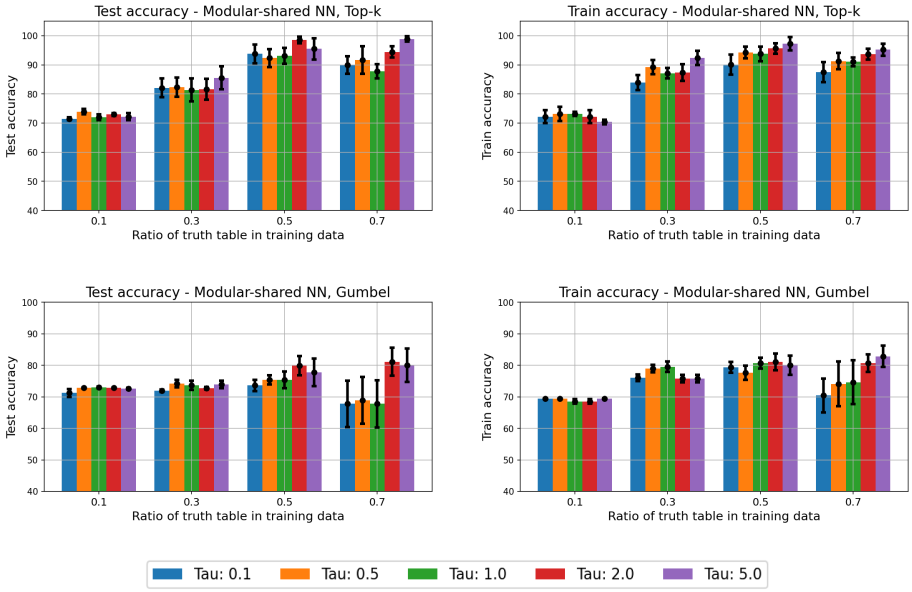

Figure 24: Train and test accuracy of *modular-shared* NNs as compared to the temperature (tau) values used for module input selection using Gumbel noise.

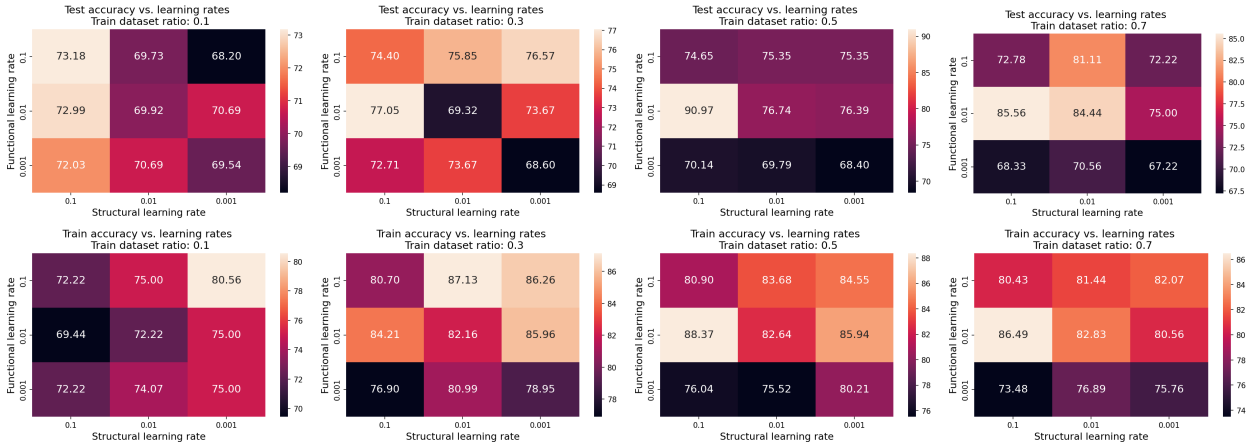

Figure 25: Test and train accuracy of *modular* NNs as compared to learning rates for structural and functional parameters. The various columns show the results for different truth table ratios for training.

Figures 25 and 26 show the training and test accuracy for various learning rates across different training sizes for the *modular* and *modular-shared* NNs, respectively. We consistently find that the best-performing combination of learning rates is 0.1 for structural parameters and 0.01 for functional parameters across both architectures. This suggests that learning inter-module connectivity and module selection requires a more aggressive optimization strategy compared to learning sub-functions within the modules. Structural parameters seem to benefit from a higher learning rate, which may be due to the need for broader exploration during training.

Moreover, larger learning rates generally improve performance on tasks involving Boolean functions. Thus, for both *modular* and *modular-shared* NNs, we focus on learning rate combinations of $\{0.1, 0.01\}$. This approach reduces the complexity of the hyperparameter search space while still achieving high performance across different training data sizes.

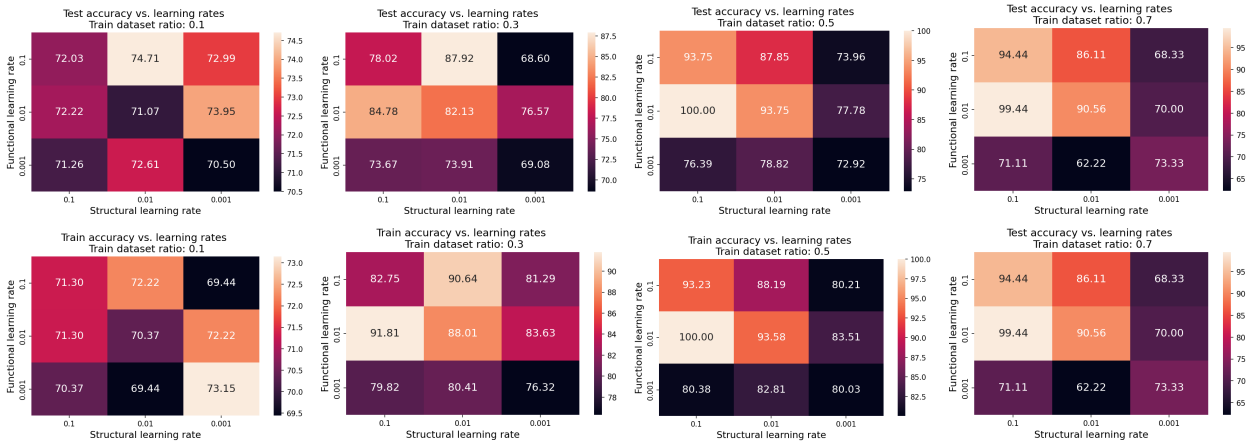

Figure 26: Test and train accuracy of *modular-shared* NNs as compared to learning rates for structural and functional parameters. The various columns show the results for different truth table ratios for training.

G Additional results: generalization and training efficiency

In this section, we present additional visualizations that provide alternative perspectives on the generalization performance and training efficiency of the various architectures.

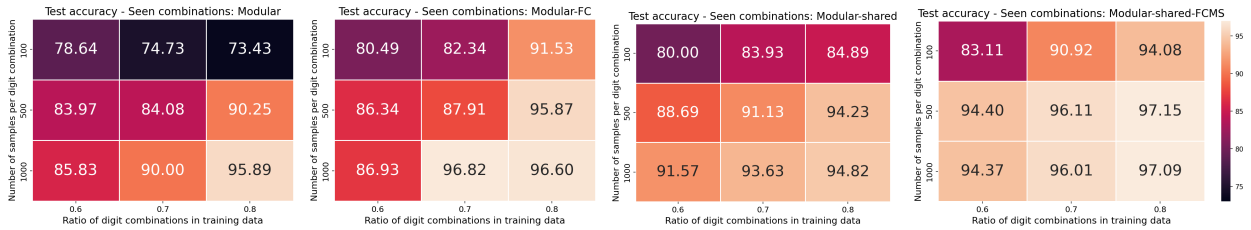

Figure 27: Generalization performance on seen combinations of different NNs trained on the hierarchically modular MNIST task, evaluated across varying proportions of digit combinations used for training and different numbers of samples per combination. Plots show results for: a. *modular* NN, b. *modular-FC* NN, c. *modular-shared* NN, and d. *modular-shared-FCMS* NN.

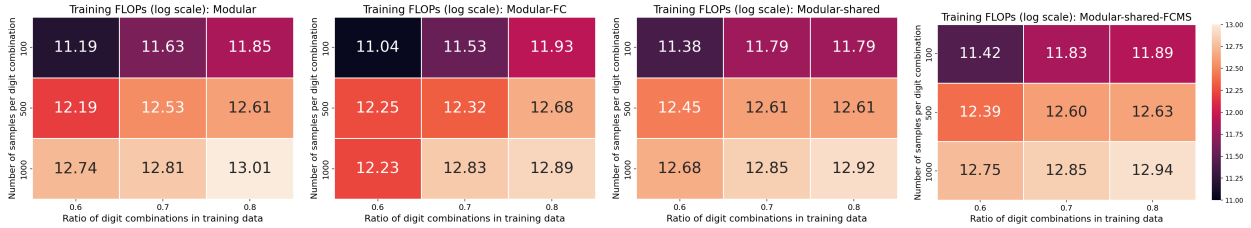

Figure 28: Training efficiency of different NNs trained on the hierarchically modular MNIST task, evaluated across varying proportions of digit combinations used for training and different numbers of samples per combination. Plots show results for: a. *modular* NN, b. *modular-FC* NN, c. *modular-shared* NN, and d. *modular-shared-FCMS* NN.

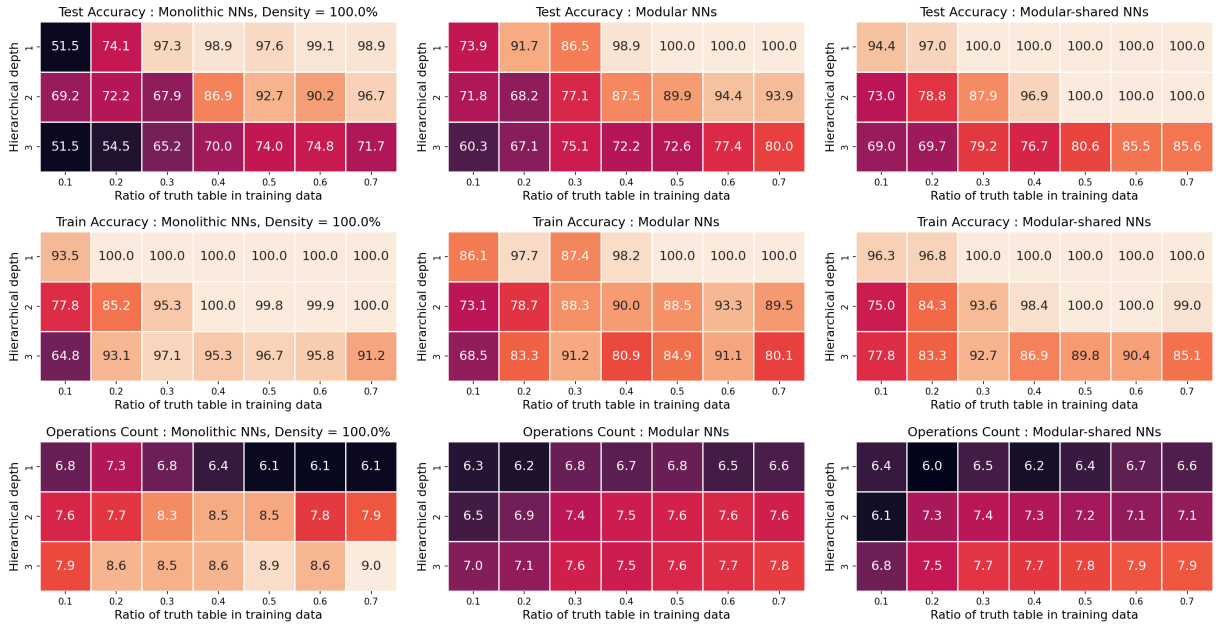

Figure 29: Test accuracy, train accuracy and FLOPs count of NNs as compared to the complexity or hierarchical depth of the Boolean function graphs and the ratio of truth table used for training. First column indicates the results for dense monolithic NNs, second column for *modular* NNs and third column for *modular-shared* NNs. We can clearly see a trend where the top right of the heatmap has better values indicating that larger training size and lower complexity functions are an easier combination to learn.